forests

MDPI

Article

Response of four tree species to changing climate in a moisture-limited area of South Siberia

Elena A. Babushkina[1], Dina F. Zhirnova[1], Liliana V. Belokopytova[1], Ivan I. Tychkov[2], Eugene A. Vaganov[2,3], KonstantinV. Krutovsky[4,5,6,7,8]*http://orcid.org/0000-0002-8819-7084

[1] Khakass Technical Institute, Siberian Federal University, 655017Abakan, Russia; babushkina70@mail.ru (E.A.B.); dina-zhirnova@mail.ru (D.F.Z.); white_lili@mail.ru (L.V.B.)
[2] Siberian Federal University, 660036 Krasnoyarsk, Russia; ivan.tychkov@gmail.com (I.I.T); eavaganov@hotmail.com (E.A.V.)
[3] Department of Dendroecology, V.N. Sukachev Institute of Forest, Siberian Branch, Russian Academy of Sciences, 660036Krasnoyarsk, Russia
[4] Department of Forest Genetics and Forest Tree Breeding, Georg-August University of Göttingen, 37077 Göttingen, Germany; konstantin.krutovsky@forst.uni-goettingen.de
[5] Center for Integrated Breeding Research, George-August University of Göttingen, 37075 Göttingen, Germany
[6] Department of Ecosystem Science and Management, Texas A&M University, College Station, TX 77840, USA
[7] Laboratory of Population Genetics, N.I. Vavilov Institute of General Genetics, Russian Academy of Sciences, 119991 Moscow, Russia
[8] Laboratory of Forest Genomics, Genome Research and Education Center, Institute of Fundamental Biology and Biotechnology, Siberian Federal University, 660036 Krasnoyarsk, Russia
* Correspondence: konstantin.krutovsky@forst.uni-goettingen.de

Received: date; Accepted: date; Published: date

Abstract: The response of vegetation to climate change is of special interest in regions where rapid warming is coupled with moisture deficit. This raises the question of the limits in plants' acclimation ability and consequent shifts of the vegetation cover. Radial growth dynamics and climatic response were studied in Scots pine (*Pinus sylvestris* L.), Siberian larch (*Larix sibirica* Ledeb.), and silver birch (*Betula pendula* Roth.) in the forest-steppe and for Siberian elm (*Ulmus pumila* L.) in the steppe of South Siberia as indicators of vegetation state and dynamics. Climate–growth relationships were analyzed by two approaches: 1) correlations between tree-ring width chronologies and short-term moving climatic series; 2) optimization of the parameters of the Vaganov-Shashkin tree growth simulation model to assess ecophysiological characteristics of species. Regional warming was accompanied with a slower increase of average moisture deficit, but not severity of droughts. In the forest-steppe, trees demonstrated a stable growth and respond to the May-July climate. In the steppe, elm is limited by moisture deficit in May–beginning of June, during peak water deficit. Forest-steppe stands are apparently acclimated successfully to the current climatic trends. It seems that elm is able to counter water deficit likely through its capacity to regulate transpiration by stomatal morphology and xylem structure, using most of stem as water reservoir, earlier onset, and high growth rate, and these physiological traits may provide advantages to this species leading to its expansion in steppes.

Keywords: climate–growth relationships; climate change; drought stress; Scots pine; Siberian elm; Siberian larch; silver birch; tree rings; Vaganov-Shashkin model

1. Introduction

The response of vegetation to climate change is the focus of many studies, especially for areas prone to drought and associated moisture deficit, where warming and stable or even decreasing precipitation can lead to an increase in the frequency and severity of droughts [1–3]. The most at risk are regions where the rate of temperature increase exceeds global trends, e.g. temperate latitudes in continental Asia: Central Asia, Mongolia, North China, and South Siberia [4–9]. For example, Liu et al. [10] reported that warming and droughts reduced growth and increased mortality for both conifers and angiosperms driving the eventual regional loss of many semi-arid forests in these regions. However, this response is not spatially uniform, and relationships between tree growth and climate should be studied also on the smaller spatial scale.

Other complication in assessment of plants' response to climatic change is due to different strategies of dealing with water stress provided by their various morphological and physiological traits. Different (isohydric and anisohydric) strategies of water balance regulation by stomatal closure [11], different hydraulic architecture of conifer, diffuse-porous, and ring-porous wood [12], possible usage of heartwood as a water storage by angiosperms [13,14], different leaf/xylem phenology and storage of non-structural carbohydrates in deciduous and evergreen species [15] are just some of internal factors affecting drought tolerance and acclimation of trees to the permanent moisture deficit.

In the Asian part of Russia, moisture deficit is typical for the semiarid steppe and forest-steppe zones of South Siberia, that stretch mainly in foothills along the plains and valleys near the southern border of Russia. A typical example of such a territory is the Khakass-Minusinsk Depression. Here, the main tree species in the forest-steppes are evergreen conifer Scots pine (*Pinus sylvestris* L.), deciduous conifer Siberian larch (*Larix sibirica* Ledeb.), and diffuse-porous angiosperm silver birch (*Betula pendula* Roth.). For all three species, the forest-steppes are the southern/lower boundary of their distribution range limited by moisture availability[16]. This forest-steppe ecotone is relatively stationary at the moment, whereas many places in the drier steppe zone are currently being overgrown by a savanna-like shrubbery consisting mainly of ring-porous angiosperm Siberian elm (*Ulmus pumila* L.). This highly drought-resistant woody species was introduced in the region in the 1960s for shelter belts, and later spread naturally to the adjacent steppe areas and abandoned farmlands (due to more than 70% reducing of sowing area in the region over the past 50 years; [17]). Its natural growth range is stretching from Central Asia through Mongolia and North China to the Far East and Korea [18]. It is the last tree species observed in the semi-deserts and even deserts (in river valleys) of Northern China [19]. Given the large magnitudes of temperature fluctuations there, this species is characterized by adequate frost resistance, although in Siberia it can be damaged by freezing during the coldest winters, which limits its distribution to the north [20].

The presence of woody plants as keystone species in both steppe and forest-steppe zones of the Khakass-Minusinsk Depression allows to use tree growth as an indicator of these semi-arid ecosystems' state and indirectly their dynamics under changing climate using dendroclimatic analysis of tree rings [21,22]. Along with the correlation models comparing climatic factors and tree growth dynamics statistically [23,24], mechanistic models can also be used to describe the explicit dependencies of growth processes on external conditions taking into account ecophysiological characteristics of plants [25–28]. An example of such modeling is the process-based Vaganov-Shashkin (VS) model of tree rings formation based on daily tree growth rate calculation from solar radiation, air temperature, and soil moisture [22]. Visual algorithm of optimization of the VS-model's parameters, i.e. search of parameters' values that provide best fit of model with actual tree growth, is successfully used to assess climatic influence and biological features of various tree species (VS-Oscilloscope) [29,30].

In this study, we attempted to answer the question of possible shifts in vegetation state and cover dynamics that may accompany current and prospective climate change in the moisture-limited zones of the Khakass-Minusinsk Depression. For that purpose, we assessed ability of acclimation to the moisture deficit and its limits for the four aforementioned tree species using two approaches. The first one was based on correlation between tree-ring width chronologies and climatic series generalized from daily data with a 21-day window and one-day step [17,31,32],

allowing us to determine the seasonality of significant climatic impacts in the growth season more precisely than classically used monthly climatic series. The second one was based on VS-modeling the dynamics of radial growth, allowing us to estimate several biophysical characteristics of individual tree species and their ability to use climatic resources in specific habitat conditions. The obtained estimates allowed us to compare the current acclimation ability of the four species and to contemplate their reaction to further regional warming.

2. Materials and Methods

2.1. Study Area and Sampling Sites

The study was conducted in the Khakass-Minusinsk Depression and foothills of the Batenevsky Ridge in the Kuznetsk Alatau mountain system (Figure 1a). The sampling was carried out mostly at one site in the vicinity of Vershino-Bidja Village near the upper reaches of the Bidja River (Table 1, Figure 2). This site was selected on the 15-20° southern slope covered with an open-canopy forest on mountain gray forest soils consisting of *Pinus sylvestris* (PISY), *Larix sibirica* (LASI), and *Betula pendula* (BEPE). Most of trees were about 50–70 years old, but several older conifer trees were also found at the site. There are abundant juvenile trees of all three species in undercover, with birch seedlings growing only in a less dense parts of the tree stand, predominantly near its lower boundary. Adjacent northern slopes were covered by more humid and dense forest stands of the same species. In the vicinity (~15 km south-east), a shelter belt near the road consisting of adult *Ulmus pumila* (ULPU) trees was selected as the second sampling site. It has a flat landscape typical for elm habitats in Khakassia, and is located amidst the crop fields and dry steppes on chernozem soils. The elm was introduced in the region only in the second half of the twentieth century, starting from urban greening and later as a part of shelter forest belts in agricultural areas [20,33].

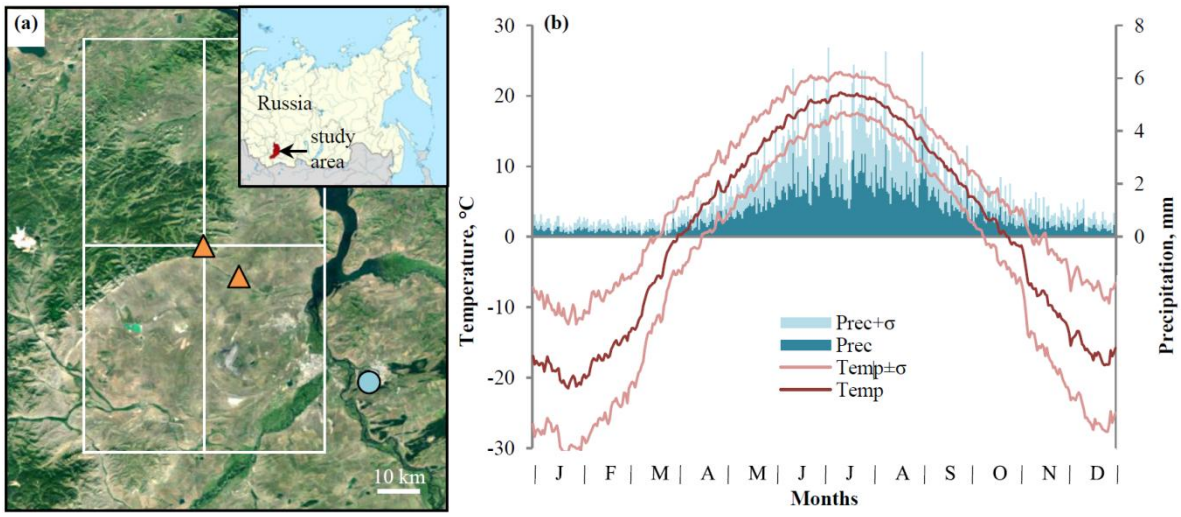

Figure 1.The study area: (**a**) a satellite map with two sampling sites marked by brown triangles and the Minusinsk weather station marked by a blue circle, respectively, area of the CRU TS grid climatic series integration (rectangles with spatial resolution of 0.5°×0.5°), and an inset map of the area location in the Asian part of Russia; (**b**) the climatic diagram of temperature (lines) and precipitation (bars) daily series (1936–2017) from the Minusinsk weather station; mean values are marked with darker shades, ranges of variation (standard deviations) are highlighted with lighter shades.

Table 1. Sampling sites and the standard tree-ring width chronologies' statistics: standard deviation (stdev), mean sensitivity coefficient (sens) [34], mean inter-serial correlation coefficient (r-bar), and expressed population signal (EPS) [35].

Species	Coordinates			Sample			Chronology			Period of EPS > 0.85	
	Latitude (N)	Longitude (E)	Altitude, m a.s.l.	Time span, years	Length, years	Number of trees/cores	stdev	sens	r-bar	Time span,	min number

											years	**of trees**
Pinus sylvestris	54°00'	90°59'	600-640	1874–2018	145	13/16	0.330	0.299	0.583	1899–2018	5
Larix sibirica	54°00'	90°59'	600-640	1750–2018	269	22/29	0.385	0.338	0.524	1900–2018	3
Betula pendula	54°00'	90°59'	600-640	1955–2017	63	15/15	0.518	0.432	0.532	1956–2017	3
Ulmus pumila	53°54'	91°11'	~310	1994–2017	24	18/30	0.229	0.294	0.563	1997–2017	6

Figure 2. Sampling sites: (**a**) mature larch tree at the main site, (**b**) mature pine tree at the main site, (**c**) general view of forest stand at the main site, (**d**) young pine trees on the forest boundary at the main site, (**e**) elm shelter belt, (**f**) steppe overgrowing with elm.

The climate of the study area is extremely continental [36] with a relatively short and hot summer, a long and cold winter and a low snow pack (Figure 1b). The average annual air

temperature is 1–1.5°C above zero. Temperatures are positive approximately from April to October (warm season). The average annual sum of precipitation is ~300–350 mm on plains and ~400 mm in the foothills, with most part of it (~90%) falling during the warm season and maximum in July. From June to September, temperature and precipitation correlate negatively (from -0.23 to -0.41, $P< 0.05$) as expected in Southern Siberia [37], leading to the frequent co-occurrences of low temperatures with much precipitation (favorable conditions), and high temperatures with little precipitation (drought) in the warm season, i.e. high variation of moisture supply.

2.2. Climatic Data

In this study we used monthly and daily series of temperature and precipitation from the Minusinsk weather station (53°41'N, 91°40'E, 251 m a.s.l.) located ~60 km south-east of the main sampling site. It has reliable monthly and daily series of the mean air temperature and the amount of precipitation over 1936-2017. Additionally, monthly series of the same climatic variables were calculated from Climate Research Unit Time-Series for 53.5-54.5°N 90.5-91.5°E area (CRU TS 4.01 [38]; Figure 1a) and compared with the Minusinsk climatic series. Correlations between grid and station temperature series are 0.91–0.98 for separate months and 0.95–0.97 for series integrated over longer periods (warm and cold season, calendar year). For precipitation series, these relationships are weaker: 0.72–0.89 and 0.79–0.81, respectively. Nevertheless, all correlations are significant at $p<0.05$, and exceed 0.85 during the warm season. It supports usage of the Minusinsk station data for the study area.

Moving series of temperature and precipitation with a 21-day window and a 1-day step were calculated from daily data, e.g. mean temperature or precipitation sum from Apr 20 to May 10, the next series covers Apr 21 – May 11, etc. This window was chosen empirically as a compromise between fine temporal scale and the stability of correlations, and during earlier studies in the region it showed adequate results for the climatic response of tree ring width [39]. Also, the Selyaninov hydrothermal coefficient (HTC = $10 \cdot \Sigma P / \Sigma T$ for T>10°C) [40] moving series with the same window and step were calculated from the same daily data from May to September, and monthly self-calibrating Palmer drought severity index (PDSI) series (grid series averaged for the same area as CRU TS data) [41] were considered as indicators of the moisture regime in the study area. The HTC series were used in detailed dendroclimatic analysis because of their finer temporal resolution, and higher sensitivity to droughts in comparison with PDSI [42]. It should be also noted that unlike HTC, PDSI has a high month-to-month correlation (0.89–0.99 for series of the consequent months) leading to lower but still significant year-to-year autocorrelation (0.34–0.44) because it depends more on the previous conditions than on the current ones.

The climatic dynamics was analyzed for seasonal series of temperature and precipitation and for monthly series of drought indices using two approaches: 1) calculation of the linear trends over the entire period of instrumental observation (1936-2017), and 2) comparison of the mean values of climatic variables between two sub-periods (1936-1976 and 1977-2017) using independent *t*-test [43] to evaluate significance of differences.

2.3. Dendrochronological Data

Wood samples (cores) were taken at the breast height from undamaged mature individual living trees within the sites described above (Table 1). Collection, transportation and processing of the cores were performed with the standard techniques of dendrochronology [23]. For each core, tree ring width (TRW) individual series was measured to the nearest 0.01 mm with LINTAB 5 platform and TSAPwin software [44]. Cross-dating of series was performed and verified in COFECHA [45]. Individual measured series of TRW were standardized in ARSTAN [46]: long-term non-climatic trends were fitted by cubic smoothing spline with a frequency response of 0.50 at 67% of the series length and removed via division of each measured TRW value by respective value of trend. Then, local standard chronologies were developed from individual standard series as a bi-weighted mean. We used the following statistical characteristics of the chronologies: standard deviation (stdev), mean sensitivity coefficient (sens)[34], mean inter-serial correlation coefficient (r-bar)[23], and expressed population signal (EPS)[35]. Climate–growth relationships were estimated by the Pearson's correlation coefficients

between TRW standard chronologies and 21-day climatic series during two sub-periods (1936–1976 and 1977–2017: T, P) to take into account climate change, and during the whole period of instrumental observations (1936–2017: HTC). During computation of the significance level of correlations, sample size was not adjusted for autocorrelation.

2.4. Tree-Ring Formation Modeling

VS-model is a process-based model that describes the formation of tree rings depending on daily climatic factors (T, P) and insolation at a particular area [22,47]. TRW is evaluated as an indexed series of the modeled general growth rate summed for the whole growth season. General growth rate is calculated as a product of three partial growth rates driven by daily mean air temperature T, soil moisture (calculated using soil features, T, P, and evapotranspiration), and solar radiation, respectively. Four temperature parameters are used to describe dependence of tree growth rate on temperature [22]. T_{min} is a minimum temperature (threshold) still allowing tree growth. The growth will stop below this temperature. T_{max} is a maximum temperature (threshold) still allowing tree growth. The growth will stop above this temperature. T_{opt1} and T_{opt2} values describe range of optimal temperatures, when growth is not limited by temperature. Then, temperature-dependent partial growth rate is estimated by piece-wise linear function, where mean daily temperature T from weather station (input data) is an independent variable:

$$Gr_T = \begin{cases} 0, & T < T_{\min} \\ (T - T_{\min}) / (T_{opt1} - T_{\min}), & T_{\min} < T < T_{opt1} \\ 1, & T_{opt1} < T < T_{opt2} \\ (T_{\max} - T) / (T_{\max} - T_{opt2}), & T_{opt2} < T < T_{\max} \\ 0, & T > T_{\max} \end{cases} \quad (1)$$

Wetness-dependent partial growth rate Gr_W is calculated in the same way, using four threshold values W_{min}, W_{opt1}, W_{opt2}, W_{max} and modeled soil moisture W as an independent variable. Light-dependent partial growth rate Gr_E is ratio of incoming daily solar radiation to its maximum value on summer solstice, calculated from the site latitude.

All numerical values of model parameters are initially estimated from species' traits and sampling site description, and then corrected by re-iterative process. In this study, a VS-Oscilloscope was used for this purpose, which is a visual parameterization tool that offers an interactive search of the optimal values of the VS-model parameters, such as optimal and extreme values of temperature and soil moisture for the growth of particular species, soil features, coefficients for transpiration rate calculation, etc. [29,30]. The criteria of optimality are estimations of the similarity between the simulated and the actual standardized tree-ring chronology, namely, their correlation and the synchronicity coefficient (the proportion of unidirectional changes of growth in actual and modeled TRW chronologies). Model parameterization was performed for each species' chronology separately.

To test model stability in a changing climate, the considered simulation period (covered by daily T and P series without missing values, i.e., 1936–2016) was divided into two sub-periods for longer chronologies of larch and pine: calibration (1970–2016) and verification (1936–1969) [23]. For shorter elm and birch chronologies, the model was calibrated along the entire chronology length without verification. Additionally, daily series and integral seasonal sums of the general and partial modeled growth rates were compared with respective seasonal climatic conditions and the actual radial growth during several years.

3. Results

3.1. Regional Climate Change

The linear time trends in seasonal climatic series show a significant ($p < 0.05$) increase of temperatures (Figure 3) during the instrumental observation period (1936–2017). This warming was

much faster during the cold season (season of negative mean monthly temperatures: November–March, 0.62°C per decade) than during the warm season (April–October, 0.13°C per decade). Overall warming of annual temperature was 0.33°C per decade. At the same time, the precipitation change was not significant, but we can note an increase of the warm season rainfall (~6.7 mm per decade). Over the same period PDSI decreased significantly (more drought). Division of observation period into two equal sub-periods (1936–1976 and 1977–2017) and comparison of their climate in finer resolution support these facts: difference between temperatures of these sub-periods is significant ($p < 0.05$) only during the cold season, and rainfall throughout the warm season except July was slightly larger in the 1977–2017 sub-period. As for drought indices, PDSI had a significantly lower mean value and variation during the second sub-period for all months. At the same time, HTC had a higher mean values for the second sub-period in June and August, a lower value in July and no significant differences in May and September.

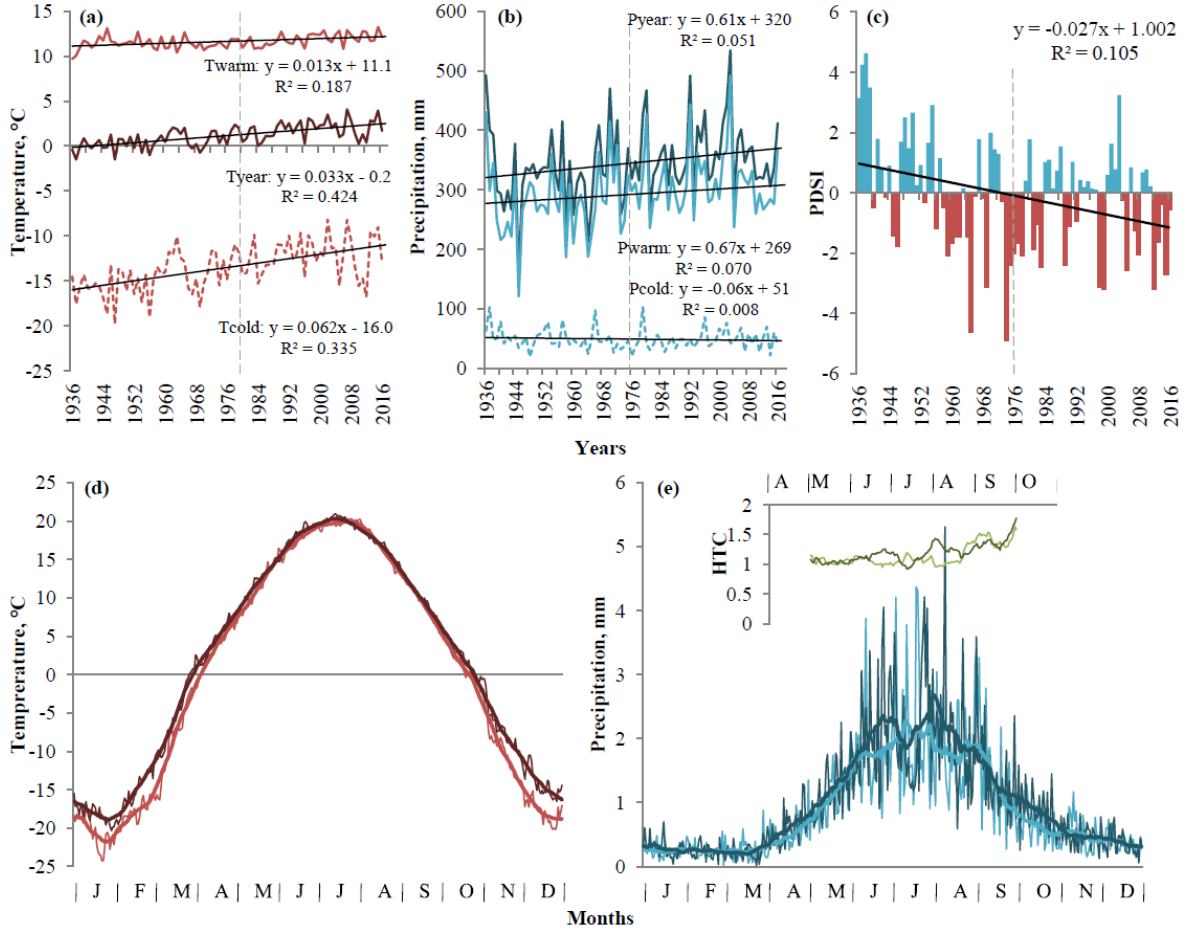

Figure 3.Climatic dynamics in the study area: (**a**) inter-annual dynamics of temperature integrated for the warm season (April–October), the cold season (November–March), and the calendar year, straight lines represent linear trends, vertical dashed line divide sub-periods; (**b**) the same plot for precipitation; (**c**) inter-annual dynamics of PDSI in July, line represents linear trend, vertical dashed line divides sub-periods; (**d**) comparison of temperature intra-annual dynamics averaged over 1936–1976 (light lines) and 1977–2017 (dark lines) sub-periods, thin lines represent daily data, thick lines represent a 21-day moving average; (**e**) the same plot for precipitation, 21-day moving series of the hydrothermal coefficient (HTC) for the same sub-periods are shown as an inset plot.

3.2. Tree-Ring Width Chronologies

Statistical characteristics of TRW standard chronologies are presented in Table 1. Presence of several older conifer trees at the main site allowed us to extend their chronologies to 145 years for pine and 269 years for larch in comparison to 63-year birch chronology. On the other hand, due to the recent introduction of the species, the oldest elm trees found in the Bidja vicinity were only

24 years old. All four species demonstrated a large variability of the radial growth, both in general (standard deviations 0.23–0.52) and in regards to year-to-year component (mean sensitivity coefficient 0.29–0.43), with the highest variation in growth of birch, and the lowest one in growth of elm. At the same time, all series contain a strong common signal, as is shown by inter-serial correlations above 0.5. The sample depth is sufficient during all period of the instrumental climatic observation for conifers, and almost all available length of broadleaf species' chronologies (EPS > 0.85; Figure 4). At the main sampling site, all three species grow in synchrony, as is evident from high correlations between their chronologies (Table 2). The highest correlation is observed between larch and birch; pine has lower correlations with other species. Elm growth dynamics is not synchronous with other species: its chronology has not significant correlations with others.

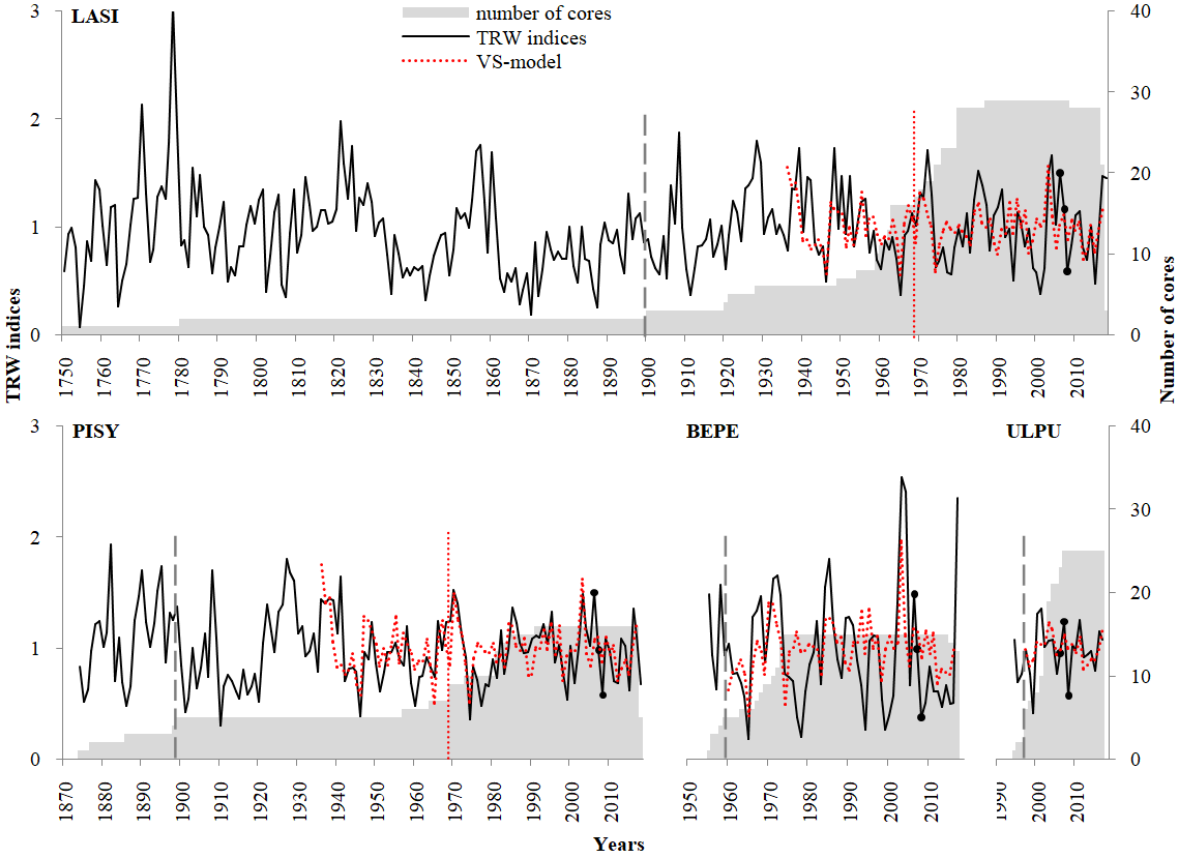

Figure 4.TRW chronologies of Siberian larch (LASI), Scots pine (PISY), silver birch (BEPE), and Siberian elm (ULPU). Black solid lines represent standard indexed chronologies; shaded area represents number of cores for each year; red dotted lines represent chronologies simulated with VS-model. For each chronology, beginning of the period when EPS > 0.85 is marked with vertical dashed line; for conifers, verification and calibration periods of modeling are divided by vertical dotted line. Years of the modeled growth rates considered in detail in Figure 6 (i.e. 2006–2008) are marked by black dots on the actual chronologies.

Table 2. Inter-species correlation coefficients between the standard TRW chronologies.

Species	*Larix sibirica*	*Pinus sylvestris*	*Betula pendula*
	1955-2017 (N = 63 years)		
Pinus sylvestris	0.677*		
Betula pendula	0.781*	0.575*	
	1994-2017 (N = 24 years)		
Pinus sylvestris	0.626*		
Betula pendula	0.775*	0.563*	
Ulmus pumila	0.116	0.288	0.184

*$P < 0.05$

3.3. Climate–Growth Relationships

Due to various lengths of chronologies, dendroclimatic analysis has some particularities: climate–growth correlations have the same reliability for conifers over both 41-year sub-periods and for birch over the second sub-period. On the other hand, one should be careful about the results for birch over the first sub-period and for elm, because their reliability is hampered by short length of series (21 year). Nevertheless, some climate–growth correlations are still significant in these cases.

The climatic response of conifers and birch is similar. The most pronounced reaction is the growth stimulation by rainfall from May to mid-July, coupled with a less strong growth limitation by temperatures of the same season (Figure 5). The hydrothermal coefficient correlates with the tree radial growth from May to mid-July. Correlations between radial growth of conifers and climatic variables are less stable and have lower values in 1936–1976 than in 1977–2017, with later onset and earlier ending of the significant response to precipitation. As for the elm chronology, its climatic reaction consists of a positive correlation with the moisture supply in May – beginning of June and a negative relationship with July temperatures. In the end of August and in September, climatic correlations of elm are reversed (positive response to temperature and negative one to precipitation and HTC). Monthly PDSI series also correlate positively with chronologies of all four species. Maximal correlations are observed in July (0.52–0.58).

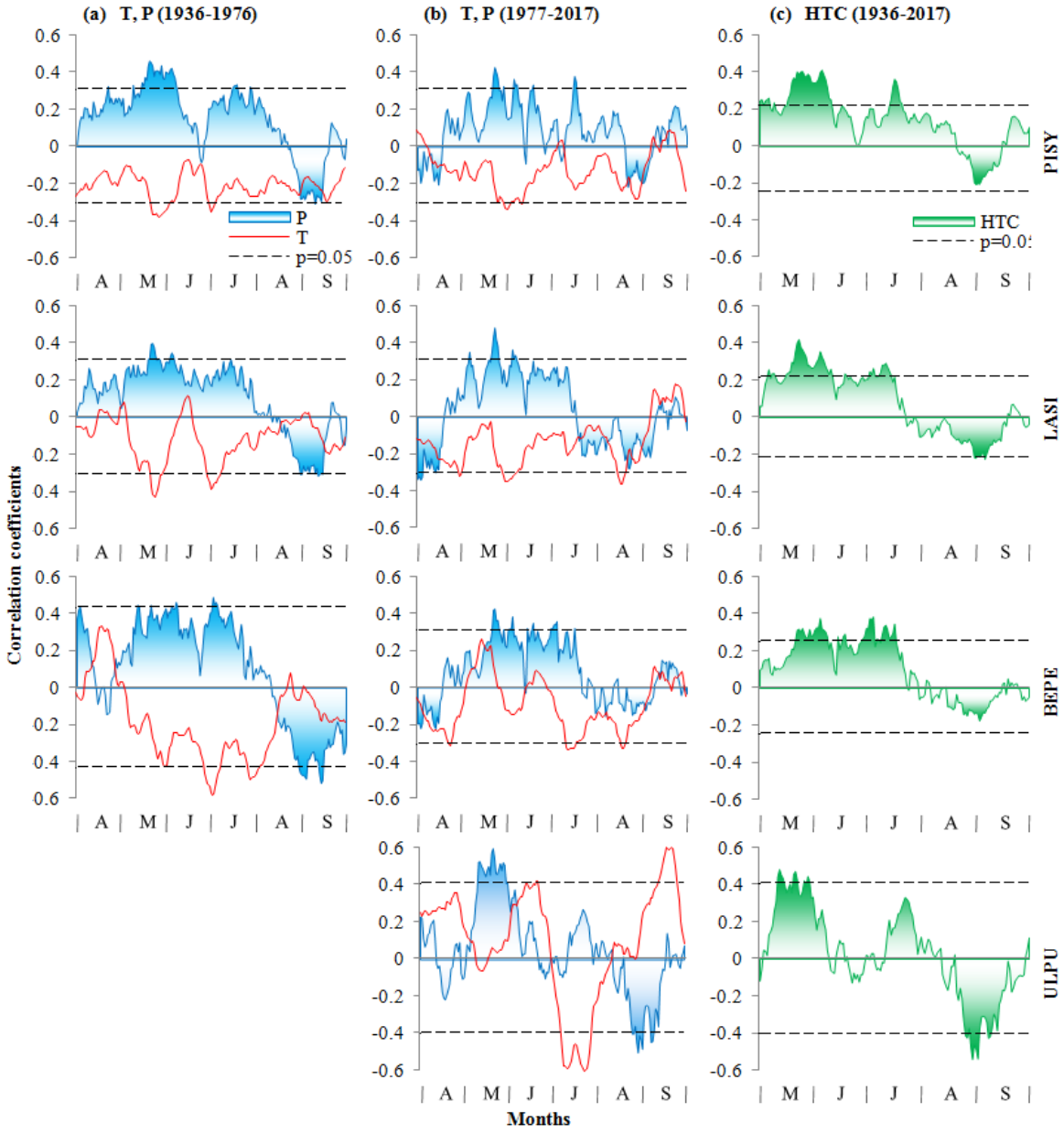

Figure 5. Correlation coefficients between TRW standard chronologies and 21-day moving series of climatic variables during April–September: (**a**) temperature (lines) and precipitation (shaded areas) for the 1936–1976 sub-period; (**b**) the same plot for the 1977–2017 sub-period; (**c**) the hydrothermal coefficient (shaded areas) for the entire 1936–2017 period. Dashed horizontal lines are thresholds for $P = 0.05$.

3.4. Growth Modeling

VS-modeling for all four species site chronologies is presented in Table 3 and Figure 4. It should be noted, that optimal parameters of the model for elm include the lowest value of minimal soil moisture and the widest range of optimal soil moisture, as well as the lowest values of coefficients for transpiration calculation (i.e. the slowest rate of transpiration). The fraction of precipitation not caught by crown is the highest for conifers and the lowest for elm. On the other hand, elm has the lowest minimum temperature threshold for growth. These parameters provide correlations between actual and modeled chronologies in the range of 0.546–0.627 over the calibration period, and 0.458–0.584 over the verification period for conifers, with the synchronicity coefficients above 65%.

Table 3. Optimal parameters and statistics of tree growth imitation VS-model for the four species.

Parameter	Description	*Pinus sylvestris*	*Larix sibirica*	*Betula pendula*	*Ulmus pumila*
T_{min}	Minimum daily temperature (low threshold) for tree growth, °C	5	5	6	1
T_{opt1}	Lower end of range of optimal daily temperatures for tree growth, °C	11	15	19	15
T_{opt2}	Upper end of range of optimal daily temperatures for tree growth, (°C)	26	24	24	25
T_{max}	Maximum daily temperature (upper threshold) for tree growth, °C	32	30	31	30
W_{min}	Minimum soil moisture (low threshold) for tree growth calculated as a ratio of water volume to soil volume	0.048	0.028	0.055	0.003
W_{opt1}	Lower end of range of optimal soil moistures for tree growth (ratio)	0.15	0.275	0.35	0.175
W_{opt2}	Upper end of range of optimal soil moistures for tree growth (ratio)	0.325	0.4	0.4	0.425
W_{max}	Maximum soil moisture (upper threshold) for tree growth (ratio)	0.675	0.65	0.525	0.55
T_{beg}	Temperature sum for initiation of growth, °C	100	90	115	105
t_{beg}	Time period for calculation of temperature sum, days	10	10	10	10
l_r	Depth of root system, mm	600	700	650	500
P_{max}	Maximum daily precipitation for saturated soil, mm/day	40	50	45	35
C_1	Fraction of precipitation penetrating soil (not caught by crown), relative unit	0.5	0.5	0.44	0.4
C_2	First coefficient for calculation of transpiration*, mm/day	0.25	0.21	0.16	0.12
C_3	Second coefficient for calculation of transpiration, relative unit per °C	0.110	0.135	0.165	0.105
	Calibration period	**1970-2017**	**1970-2017**	**1960-2016**	**1997-2017**
R	Correlation between model and actual series	0.627	0.594	0.619	0.546
R^2	Coefficient of determination	0.394	0.352	0.383	0.298
Synch	Synchronicity between model and actual series, %	72.9	72.3	64.9	76.2
	Verification period	**1936-1969**	**1936-1969**		
R	Correlation between model and actual series	0.584	0.458		
R^2	Coefficient of determination	0.342	0.210		
Synch	Synchronicity between model and actual series, %	73.5	67.6		

*In VS-model, transpiration is calculated from daily growth rate and temperature with simplified equation: $C_2 \cdot Gr \cdot \exp(C_3 \cdot T)$.

Daily series of external conditions and modeled growth rates in comparison with actual tree rings for all four species were considered on the example of 2006–2008. For more than 75% of individual trees of each species, during these years TRW series have pattern of the widest ring in 2006 and the narrowest one in 2008 (Figure 6a). This pattern is also observed in both earlywood and latewood of the wide rings of pine and elm, and only in earlywood of the narrow rings of birch and

309 larch. Anomalies of wood anatomy were not observed during these years for any species. Weather of
310 these years is characterized by the following patterns: 2006 – late but warm beginning of the growth
311 season, high soil moisture during the most of summer except the end of June; 2007 – early beginning
312 of the growth season, wet and cool May–June, dry and warm July and August; 2008 – warm summer
313 with droughts in the first half of June and from mid-July (Figure 6b). The modeled dynamics of tree
314 growth shows a slower growth rate for larch and birch, a medium growth rate with severe
315 intra-seasonal depressions (deviations from the maximal growth rate curve controlled by solar
316 radiation) for pine, and the fastest growth rate with minimal depressions for elm (Figure 6c), which
317 is consistent with actual TRW. The comparison of years shows that the modeled growth rates for all
318 species have maxima in May – beginning of June and mid-July in 2006, June in 2007, and beginning
319 of July in 2008. At the same time, interannual pattern of wide–medium–narrow rings observed in the
320 actual TRW in 2006-2008 is not present in the dynamics of integral sums of the modeled general
321 growth rate, but only in its moisture-dependent component (Figure 6d).

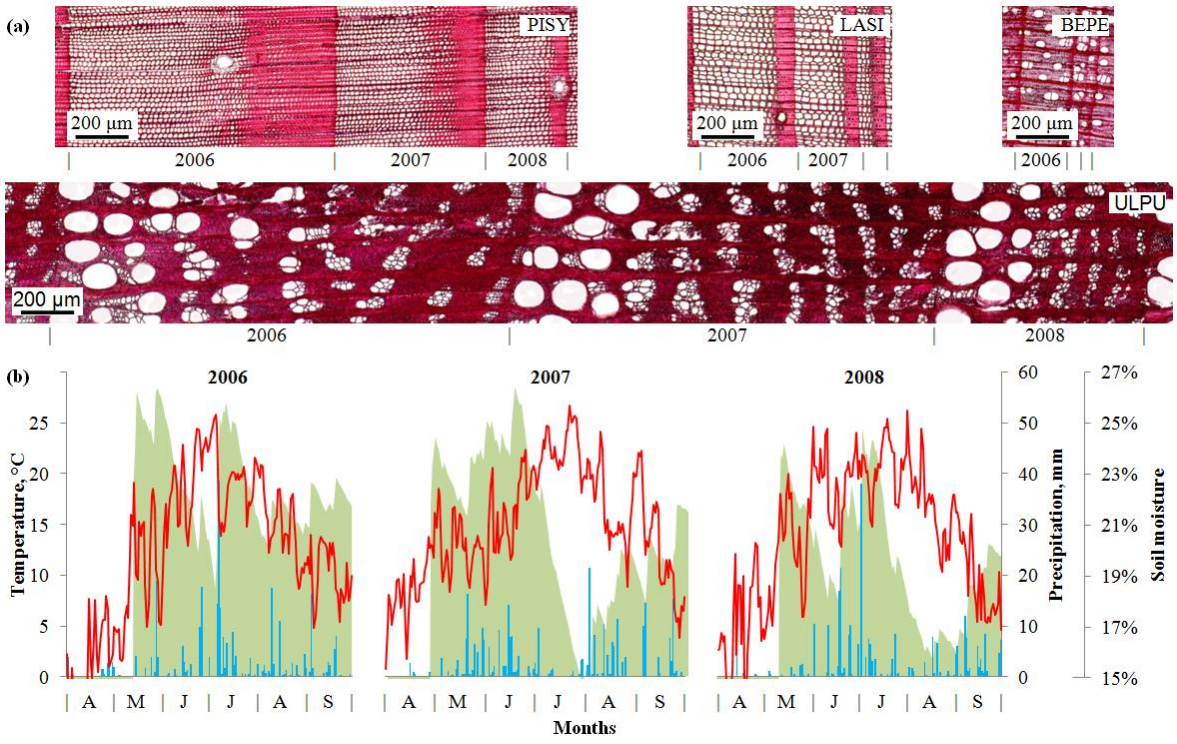

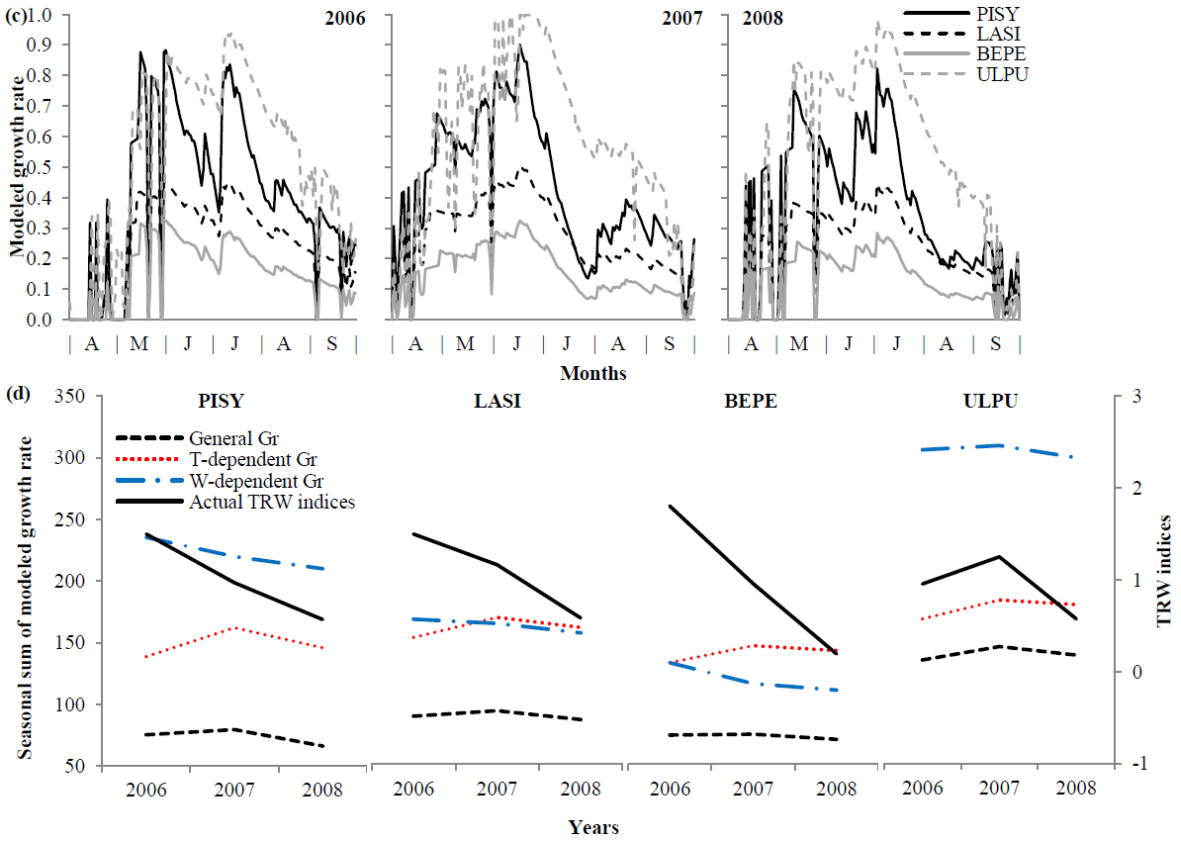

Figure 6.Growth patterns of the four considered species and external conditions during 2006–2008: (**a**) examples of tree rings' cell structure microphotographs; (**b**) daily dynamics of temperature (lines) and precipitation (bars) during April–September, and modeled soil moisture (shaded areas), averaged for all considered species starting from the modeled onset of radial growth; (**c**) the modeled daily series of general growth rate (in a unit share, i.e. a fraction of maximal growth rate) for each species; (d) the total seasonal sum of the modeled growth rates (Gr, in a unit share): general growth rate (black dashed lines), temperature-dependent partial growth rate (dotted lines), wetness-dependent partial growth rate (dot dash lines), and actual TRW indices (solid lines).

4. Discussion

4.1.Growth Patterns of Considered Species

The sensitivity and variation of considered species' chronologies in the study area are in good agreement with their ranking by the drought tolerance (elm–pine–larch–birch in decreasing order [48,49]). On the other hand, the sensitivity coefficient of the elm chronology can also be reduced by its young age, as many researchers have noted an age-related increase in the climatic sensitivity of tree growth [50-52]. The greater similarity between the dynamics of larch and birch growth is most likely due to physiological and phenological differences of evergreen pine due to the presence of foliage at the growth season onset and subsequent absence of a delay in cambium activation [15]. Unlike many other drought-limited areas in the continental Asia, there are no sharply decreasing trends in tree radial growth and high tree mortality in the study area during several last decades, probably due to positive trend of precipitation partially compensating for climate warming and thus slower increase of PDSI [10].

While the study area is the southern/lower border of the distribution range for both conifers and birch, the opposite is observed for elm, since its natural range is located in the more arid steppes and semi-deserts. Therefore, this is likely the reason why its growth dynamics is asynchronous with the other species.

4.2.Climatic Response and Growth Modeling of Trees

In general, the combination of a positive precipitation effect on tree growth and a weaker negative impact of temperature during the first half of the growing season is typical for semiarid areas of the region [54,55]. It should be noted that this reaction is coherent for all three species growing at the main sampling site indicating similar degree of drought tolerance and a strategy of acclimation to the moisture deficit. Regarding possible change of climatic response due to increased temperatures, moisture limitation of tree growth in the forest-steppe has not changed significantly over recent decades. This may be due to the fact that the temperature increase is relatively slow during the growth season and may be compensated by a positive trend in precipitation, and the decreased mean PDSI is compensated by its lesser variation (i.e. absence of extreme droughts in the second sub-period).

Ulmus pumila is one of the most xerophytic elm species [18,56], and its strategy of acclimation in moisture-limited regions is based on several anatomical features and physiological mechanisms. Despite the very large vessels that are potentially more vulnerable to cavitation, elm has effective phenotypic regulation of transpiration at the level of stomatal morphology [57]. As in a typical ring-porous tree, sap flows mainly through the earlywood vessels of the last ring, and the contribution of the preceding rings does not exceed 10% [58,59], primarily due to losing hydraulic conductivity of very large earlywood vessels in winter [60]. Probably, it provides a greater extent of elm acclimation to the current season conditions by high plasticity of the hydraulic structure, first of all during formation of earlywood. On the other hand, heartwood of elm (i.e. most of its trunk volume) serves as a water storage (cf. other angiosperm species [13,14]). This feature differs significantly from the considered conifers, which have a wider proportion of sapwood [61,62] (cf. also observation of the last ring accounting for only 15–20% of hydraulic conductivity of Scots pine [63]), whereas birch does not form heartwood at all. Differences of elm hydraulic strategy possibly lead to concentration of its response to precipitation and HTC in the beginning of the growth season, when earlywood is forming. If moisture supply is sufficient at this time, excessive water can be reserved in the heartwood and used later for mitigating the effects of moisture deficit. Also, possible onset of growth at the lower temperatures (~1°C) gives elm an advantage of using snowmelt water. On the other hand, as the seasonal dynamics of HTC shows, droughts in the study area occur more frequently in May–early June. Therefore, it is possible that later in the season conditions are usually not extreme enough to cause a water stress and a significant growth response in elm, which is supported by difference in the optimal values of the VS-model parameters and the less pronounced depression of the growth rate due to soil moisture decrease (Figure 6). A negative reaction to July temperatures may be caused by heat stress. The reverse climatic response of elm in August–September, when moisture supply is usually maximal (more precipitation and higher HTC), can be caused by its low tolerance to excessive soil moisture [18,20]. But there is an open question if these correlations have an ecological meaning, because at that time of season the radial growth is mostly finished [59].In general, the significant climatic impact on the elm growth in the study area has shorter seasonal windows compared to the other considered species, which also gives it an advantage, because there are time intervals in the warm season when moisture deficit can suppress growth of native species, but not elm.

Despite different seasonality of climatic response, regulation of the radial growth by the soil moisture content is common for all four species. It is supported by their strong response to PDSI in July, which due to its high month-to-month autocorrelation can be considered as an integral characteristic of water supply during most period of the tree ring formation. Weakening of the response to all climatic variables in August indicates that cambial activity terminates near the end of July – beginning of August for all tree species in the study area, but after that TRW still can register climatic influence to the lesser extent – via expansion of cells.

It was shown before that in the dry environment the onset of xylogenesis is regulated by both temperature threshold and moisture supply [64]. Later, both growth rate during the season and timing of the growth cessation are regulated by water deficit [65]. VS-model takes into consideration the temperature threshold explicitly as one of its parameters (T_{beg} in Table 3), and includes growth suppression by drought throughout the season. However, moderate correlations between actual and

modeled tree growth show that the algorithm used for describing climate–growth relationships and phenology of xylogenesis in VS-model is not conclusive yet and can be further improved. E.g., the comparison of growth rates for 2006–2008 suggests that probably, a contribution of moisture limitation in the growth rate should be increased, and new parameters should be defined for the cessation of growth.

4.3.Prospects of Tree Stands Dynamics Under Climate Change

The smaller size, less shade- and drought-tolerant nature of birch can lead to its gradual displacement to the margins and open parts of the stand. This is supported by observed currently absence of birch seedlings in close-canopy parts of the stand. The appreciable warming during winter months can also have a positive effect on the tree growth, reducing the likelihood of injuries due to frost in winter and carbohydrates cost for the restoration of hydraulic conductivity in spring. This effect is stronger for angiosperms, especially for ring-porous elm [12]. In addition, the increase in the moisture deficit during recent decades has been rather slow, which allows forest stands in the forest-steppe zone to adapt successfully to the new climatic averages.

Despite a low possibility to observe climate change effects on elm growth directly due to the short length of the chronology, it is expected that the winter temperature increase will have a positive effect on elm, contributing to the spread of this species through overgrowing of steppes and abandoned farmland (Figure 2f), and the relatively high rate of this process can be ensured through a short reproductive cycle and high migratory ability of this species (abundant fruiting and wind-dispersion of very light seeds).

5. Conclusions

The study showed that warming is partially compensated by the increased precipitation in the studied region. This compensation slowed down increase in the climate aridity allowing pine, larch, and birch to successfully acclimate to the current conditions in the forest-steppe zone. Acclimation is confirmed by data of the dendroclimatic analysis and the modeling of tree rings. In more arid steppe conditions, the anatomical and morphological features of elm give it advantages contributing to the rapid replacement of steppe vegetation with savanna-like shrubs of this species.

Author Contributions: conceptualization, E.A.B. and E.A.V.; methodology, E.A.V.; software, I.I.T.; validation, E.A.V. and K.V.K.; formal analysis, L.V.B. and I.I.T.; investigation, D.F.Z.; resources, E.A.B. and D.F.Z.; data curation, L.V.B.; writing—original draft preparation, E.A.B., D.F.Z. and L.V.B.; writing—review and editing, L.V.B., D.F.Z. and K.V.K.; visualization, L.V.B.; supervision, E.A.V.; project administration, E.A.B. and K.V.K.; funding acquisition, E.A.V. and K.V.K.

Funding: This research was funded by the Russian Science Foundation, grant numbers19-18-00145 (“Modeling of the mutual impact of climate change processes and the development of the forestry economy: case-study of Siberian regions” PI: E.A.V.) and 19-14-00120 (“Study of genetic adaptation of trees to stress environmental factors on the basis of genome-wide and dendrochronological analysis in the context of global climate change” PI: K.V.K), and by the Ministry of Science and Higher Education of the Russian Federation, Program "Science of Future", project number 5.3508.2017/4.6 (PI: V.V.S.).

Conflicts of Interest: The authors declare no conflict of interest. The funders had no role in the design of the study; in the collection, analyses, or interpretation of data; in the writing of the manuscript, or in the decision to publish the results.

References

1. Dai, A.; Trenberth, K.E.; Karl, T.R. Global variations in droughts and wet spells: 1900–1995. *Geophys. Res. Lett.***1998**, *25*, 3367–3370. htpps://doi.org/10.1029/98GL52511.
2. Dulamsuren, C.; Khishigjargal, M.; Leuschner, C.; Hauck, M. Response of tree-ring width to climate warming and selective logging in larch forests of the Mongolian Altai. *J. Plant Ecol.***2014**, *7*, 24–38. htpps://doi.org/10.1093/jpe/rtt019.

3. Flanagan, P.X.; Basara, J.B.; Xiao, X. Long-term analysis of the asynchronicity between temperature and precipitation maxima in the United States Great Plains. *Int. J. Climatol.***2017**, *37*, 3919–3933. htpps://doi.org/10.1002/joc.4966.
4. Rogers, J.C.; Mosely-Thompson, E. Atlantic Arctic cyclones and mild Siberian winters of the 1980s. *Geophys. Res. Lett.***1995**, *22*, 799–802. htpps://doi.org/10.1029/95GL00301.
5. Savelieva, N.I.; Semiletov, I.P.; Vasilevskaya, L.N.; Pugach, S.P. A climate shift in seasonal values of meteorological and hydrological parameters for Northeastern Asia. *Prog. Oceanogr.***2000**, *47*, 279–297. htpps://doi.org/10.1016/S0079-6611(00)00039-2.
6. Davi, N.K.; Jacoby, G.C.; Curtis, A.E.; Baatarbileg, N. Extension of drought records for central Asia using tree rings: west-central Mongolia. *J. Clim.***2006**, *19*, 288–299. htpps://doi.org/10.1175/JCLI3621.1.
7. IPCC Climate Change. *The Physical Science Basis. Contribution of Working Group I to the Fifth Assessment Report of the Intergovernmental Panel on Climate Change*; Stocker, T.F., Qin, D., Plattner, G.K., Tignor, M., Allen, S.K., Boschung, J., Nauels, A., Xia, Y., Bex, V., Midgley, P.M., Eds.; Cambridge University Press: Cambridge, UK, 2013; p. 1535.
8. Kattsov, V.M.; Semenov, S.M., Eds. *Second Roshydromet assessment report on climate change and its consequences in Russian Federation*; Roshydromet, Moscow, Russia, 2014; p. 54.
9. Liu, X.; Pan, Y.; Zhu, X.; Yang, T.; Bai, J.; Sun, Z. Drought evolution and its impact on the crop yield in the North China Plain. *J. Hydrol.* **2018**, *564*, 984–996. htpps://doi.org/10.1016/j.jhydrol.2018.07.077.
10. Liu, H.; Park Williams, A.; Allen, C.D.; Guo D.; Wu, X.; Anenkhonov, O.A.; Liang, E.; Sandanov, D.V.; Yin, Y.; Qi, Z.; Badmaeva, N.K. Rapid warming accelerates tree growth decline in semi-arid forests of Inner Asia. *Glob. Change Biol.***2013**, *19*, 2500–2510. htpps://doi.org/10.1111/gcb.12217.
11. McDowell, N.; Pockman, W.T.; Allen, C.D.; Breshears, D.D.; Cobb, N.; Kolb, T.; Plaut, J.; Sperry, J.; West, A.; Williams, D.G.; Yepez, E.A. Mechanisms of plant survival and mortality during drought: why do some plants survive while others succumb to drought? *New Phytol.***2008**, *178*, 719–739. https://doi.org/10.1111/j.1469-8137.2008.02436.x.
12. Carnicer, J.; Barbeta, A.; Sperlich, D.; Coll, M.; Peñuelas, J. Contrasting trait syndromes in angiosperms and conifers are associated with different responses of tree growth to temperature on a large scale. *Front. Plant Sci*. **2013**, *4*, 409. htpps://doi.org/10.3389/fpls.2013.00409.
13. Matheny, A.M.; Bohrer, G.; Garrity, S.R.; Morin, T.H.; Howard, C.J.; Vogel, C.S. Observations of stem water storage in trees of opposing hydraulic strategies. *Ecosph.***2015**, *6*, 1–13. htpps://doi.org/10.1890/ES15-00170.1.
14. Hu, G.; Liu, H.; Shangguan, H.; Wu, X.; Xu, X.; Williams, M. The role of heartwood water storage for semi-arid trees under drought. *Agric. For. Meteorol.***2018**, *256-257*, 534–541. htpps://doi.org/10.1016/j.agrformet.2018.04.007.
15. Piper, F.I.; Fajardo, A. Foliar habit, tolerance to defoliation and their link to carbon and nitrogen storage. *J. Ecol.***2014**, *102*, 1101–1111. https://doi.org/10.1111/1365-2745.12284.
16. Nazimova, D.I.; Polikarpov, N.P. Forest zones of Siberia as determined by climatic zones and their possible transformation trends under global change. *Silva Fenn.***1996**, *30*, 201–208. htpps://doi.org/10.14214/sf.a9232.
17. Babushkina, E.A.; Belokopytova, L.V.; Zhirnova, D.F., Shah, S.K.; Kostyakova, T.V. Climatically driven yield variability of major crops in Khakassia (South Siberia). *Int. J. Biometeorol.***2018**, *62*, 939–948. htpps://doi.org/10.1007/s00484-017-1496-9.
18. Wang, C.W. *The forests of China, with a survey of grassland and desert vegetation*; Harvard University, Cambridge, UK, 1961.
19. Wesche, K.; Walther, D.; VonWehrden, H., Hensen, I. Trees in the desert: Reproduction and genetic structure of fragmented *Ulmus pumila* forests in Mongolian drylands. *Flora Morphol. Distrib. Funct. Ecol. Plants***2011**, *206*, 91–99. htpps://doi.org/10.1016/j.flora.2010.01.012.
20. Mamyshev, K.V., Biology and morphological characteristics of *Ulmus pumila* L. in the system of belts Uybat steppe. *Theor. Appl. Sci.***2014**, *3*, 76–80.
21. Fritts, H.C. *Tree rings and climate*; Academic Press, London, UK, 1976.
22. Vaganov, E.A.; Hughes, M.K.; Shashkin, A.V. *Growth dynamics of conifer tree rings: images of past and future*; Springer, Berlin, Germany, 2006.
23. Cook, E.R.; Kairiukstis, L.A. *Methods of Dendrochronology: Applications in the Environmental Sciences*; Springer, Dordrecht, 1990. htpps://doi.org/10.1007/978-94-015-7879-0.

24. Hughes, M.K.; Swetnam, T.W.; Diaz, H.F., Eds. *Dendroclimatology: Progress and Prospects*; Springer, New York, USA, Netherlands, 2010.
25. Misson, L. MAIDEN: a model for analyzing ecosystem processes in dendroecology. *Can. J. For. Res.***2004**, *34*, 874–887. htpps://doi.org/10.1139/x03-252.
26. Dufrene, E.; Davi, H.; Francois, C.; le Maire, G.; Le Dantec V.; Granier, A. Modelling carbon and water cycles in a beech forest. Part I: model description and uncertainty analysis on modelled NEE. *Ecol. Modell.***2005**, *185*, 407–436. htpps://doi.org/10.1016/j.ecolmodel.2005.01.004.
27. Buckley, L.B.; Urban, M.C.; Angilletta, M.J.; Crozier, L.G.; Rissler, L.J.; Sears, M.W. Can mechanism inform species' distribution models? *Ecol. Lett.***2010**, *13*, 1041–1054. htpps://doi.org/10.1111/j.1461-0248.2010.01479.x.
28. Drew, D.M.; Downes, G.M.; Battaglia, M. CAMBIUM, a process-based model of daily xylem development in *Eucalyptus*. *J. Theor. Biol.***2010**, *264*, 395–406. htpps://doi.org/10.1016/j.jtbi.2010.02.013.
29. Shishov, V.V.; Tychkov, I.I.; Popkova M.I.; Ilyin, V.A.; Bryukhanova, M.V.; Kirdyanov, A.V. VS-oscilloscope: a new tool to parameterize tree radial growth based on climate conditions. *Dendrochronologia***2016**, *39*, 42–50. htpps://doi.org/ 10.1016/j.dendro.2015.10.001.
30. Tychkov, I.I.; Sviderskaya, I.V.; Babushkina, E.A.; Popkova, M.I.; Vaganov, E.A.; Shishov, V.V. How can the parameterization of a process-based model help us understand real tree-ring growth? *Trees***2019**, *33*, 345–357. htpps://doi.org/10.1007/s00468-018-1780-2.
31. Liang, W.; Heinrich, I.; Simard, S.; Helle, G.; Dorado Linan; I., Heinken, T. Climate signals derived from cell anatomy of Scots pine in NE Germany. *Tree Physiol.***2013**, *33*, 833–844. htpps://doi.org/10.1093/treephys/tpt059.
32. Carrer, M.; Castagneri, D.; Prendin, A.L.; Petit, G.; von Arx, G. Retrospective analysis of wood anatomical traits reveals a recent extension in tree cambial activity in two high-elevation conifers. *Front. Plant Sci.***2017**, *8*, 737. htpps://doi.org/10.3389/fpls.2017.00737.
33. Lobanov, A.I.; Varaksin, G.S. Effect of seeding method and microtopography on vegetation and condition of Siberian elm stands in shelter forest belts of arid steppe zone of Khakassia. *For. J.***2012**, *2*, 28–34.
34. Shiyatov, S.G. *Dendrochronology of the higher timberline on the Urals*; Nauka, Moscow, Russia, 1986.
35. Wigley, T.M.L.; Briffa, K.R.; Jones, P.D. On the average value of correlated time series, with applications in dendroclimatology and hydrometeorology. *J. Appl. Meteorol. Climatol.***1984**, *23*, 201-213. htpps://doi.org/10.1175/1520-0450(1984)023%3C0201:OTAVOC%3E2.0.CO;2.
36. Alisov, B.P. *Climate of the USSR*; Moscow State University, Moscow, Russia, 1956.
37. Bazhenova, O.I.; Tyumentseva, E.M. The structure of contemporary denudation in the steppes of the Minusinskaya depression. *Geogr. Nat. Resour.***2010**, *31*, 362–369. htpps://doi.org/10.1016/j.gnr.2010.11.010.
38. Harris, I.; Jones, P.D.; Osborn, T.J.; Lister, D.H. Updated high-resolution grids of monthly climatic observations – the CRU TS3.10 Dataset. *Int. J. Climatol.***2014**, *34*, 623–642. htpps://doi.org/10.1002/joc.3711.
39. Babushkina, E.; Belokopytova, L.; Zhirnova, D.; Barabantsova, A.; Vaganov, E. Divergent growth trends and climatic response of *Picea obovata* along elevational gradient in Western Sayan Mountains, Siberia. *J. Mt. Sci.***2018**, *15*, 2378–2397. htpps://doi.org/10.1007/s11629-018-4974-6.
40. Selyaniniov, G.T. Principles of agroclimatic regional planning in USSR; In *Questions of agroclimatic zoning of the USSR*; Davitaya, F.F., Shulgina, A.I., Eds.; Ministry of Agriculture of the USSR, Moscow, Russia, 1958; pp. 18–26.
41. van der Schrier, G.; Barichivich, J.; Briffa, K.R.; Jones, P.D. A scPDSI-based global data set of dry and wet spells for 1901–2009. *J. Geophys. Res.: Atmos.***2013**, *118*, 4025–4048. htpps://doi.org/10.1002/jgrd.50355.
42. Cherenkova, E.A.; Zolotokrylin, A.N. On the comparability of some quantitative drought indices. *Fundam.Appl. Climatol.***2016**, *2*, 79–94. htpps://doi.org/10.21513/2410-8758-2016-2-79-94.
43. Rice, J.A. *Mathematical statistics and data analysis*. 3rd ed. Cengage Learning: Independence, USA, 2006.
44. Rinn, F. *TSAP-Win: Time series analysis and presentation for dendrochronology and related applications: User reference*; RINNTECH, Heidelberg, Netherlands, 2003.
45. Holmes, R.L. Computer-assisted quality control in tree-ring dating and measurement. *Tree-Ring Bull.***1983**, *43*, 68–78.
46. Cook, E.R.; Krusic, P.J. *Program ARSTAN: a tree-ring standardization program based on detrending and autoregressive time series modeling, with interactive graphics*; Lamont-Doherty Earth Observatory, Columbia University, Palisades, USA, 2005.

47. Vaganov, E.A.; Anchukaitis, K.J.; Evans, M.N. How well understood are the processes that create dendroclimatic records? A mechanistic model of the climatic control on conifer tree-ring growth dynamics; In *Dendroclimatology: Progress and Prospects*; Hughes, M.K., Swetnam, T.W., Diaz, H.F., Eds.; Springer, New York, USA, 2011; pp. 37–75.
48. Chetin, Y.I. Features of growth and drought tolerance of larch, pine, spruce and birch in cultures of the agroforestmeliorative zone of Western Siberia. In *Works on Forestry of Siberia*, Proceedings of the Conference on Rationalization of Siberian Forestry, Novosibirsk, Russia, 12-15 Sep. 1957; AS USSR: Novosibirsk, Russia, **1958**; 4, pp. 328–338.
49. Niinemets, Ü.; Valladares, F. Tolerance to shade, drought, and waterlogging of temperate Northern Hemisphere trees and shrubs. *Ecol. Monogr.***2006**, *76*, 521–547. https://doi.org/10.1890/0012-9615(2006)076[0521:TTSDAW]2.0.CO;2.
50. Carrer, M.; Urbinati, C. Age-dependent tree-ring growth responses to climate in *Larix decidua* and *Pinus cembra*. *Ecol.***2004**, *85*, 730–740. htpps://doi.org/10.1890/02-0478.
51. Esper, J., Niederer, R., Bebi, P., Frank, D., Climate signal age effects – evidence from young and old trees in the Swiss Engadin. *For. Ecol. Manag.***2008**, *255*, 3783–3789. htpps://doi.org/10.1016/j.foreco.2008.03.015.
52. Dorado Linan, I.; Gutiérrez, E.; Heinrich, I.; Andreu-Hayles, L.; Muntán, E.; Campelo, F.; Helle, G. Age effects and climate response in trees: a multi-proxy tree-ring test in old-growth life stages. *Eur. J. For. Res.***2012**, *131*, 933–944. htpps://doi.org/10.1007/s10342-011-0566-5.
53. Kraus, C.; Zang, C.; Menzel, A. Elevational response in leaf and xylem phenology reveals different prolongation of growing period of common beech and Norway spruce under warming conditions in the Bavarian Alps. *Eur. J. For. Res.***2016**, *135*, 1011–1023. htpps://doi.org/10.1007/s1034 2-016-0990-7.
54. Babushkina, E.A.; Vaganov, E.A.; Belokopytova, L.V.; Shishov, V.V.; Grachev, A.M. Competitive strength effect in the climate response of Scots pine radial growth in south-central Siberia forest-steppe. *Tree Ring Res.***2015**, *71, 106–117.* htpps://doi.org/10.3959/1536-1098-71.2.106.
55. Babushkina, E.A.; Belokopytova, L.V.; Shah, S.K.; Zhirnova, D.F. Past crops yield dynamics reconstruction from tree-ring chronologies in the forest-steppe zone based on low- and high-frequency components. *Int. J. Biometeorol.***2018,** *62,* 861–871. htpps://doi.org/10.1007/s00484-017-1488-9.
56. Ghelardini, L. *Bud burst phenology, dormancy release and susceptibility to Dutch elm disease in elms (Ulmus spp.):* Dissertation; Swedish University of Agricultural Sciences, Uppsala, Sweden, 2007.
57. Park, G.E.; Lee, D.K.; Kim, K.W.; Batkhuu, N.O.; Tsogtbaatar, J.; Zhu, J.J.; Jin, Y.; Park, P.S.; Hyun, J.O.; Kim, H.S. Morphological characteristics and water-use efficiency of Siberian elm trees (*Ulmus pumila* L.) within arid regions of northeast Asia. *For.***2016**, *7*, 280. htpps://doi.org/10.3390/f7110280.
58. Tyree, M.T.; Zimmermann, M.H. *Xylem structure and the ascent of sap*; Springer-Verlag, Berlin, Germany, 2002.
59. Solla, A.; Martín, J.A.; Corral, P.; Gil, L. Seasonal changes in wood formation of *Ulmus pumila* and *U. minor* and its relation with Dutch elm disease. *New Phytol.***2005**, *166*, 1025–1034. htpps://doi.org/10.1111/j.1469-8137.2005.01384.x.
60. Cochard, H.; Tyree, M.T. Xylem dysfunction in *Quercus*: vessel sizes, tyloses, cavitation and seasonal changes in embolism. *Tree Physiol.***1990**, *6*, 393–407. htpps://doi.org/10.1093/treephys/6.4.393.
61. Wang, X.; Wang, C.; Zhang, Q.; Quan, X. Heartwood and sapwood allometry of seven Chinese temperate tree species. *Ann. For. Sci.***2010**, *67*, 410. htpps://doi.org/10.1051/forest/2009131.
62. Millers, M. The proportion of heartwood in conifer (*Pinus sylvestris* L., *Picea abies* [L.] H. Karst.) trunks and its influence on trunk wood moisture. *J. For. Sci.* **2013**, *59*, 295–300.
63. Urli, M.; Porté, A.J.; Cochard, H.; Guengant, Y; Burlett, R.; Delzon, S. Xylem embolism threshold for catastrophic hydraulic failure in angiosperm trees. *Tree Physiol.* **2013,***33*, 672–683. htpps://doi.org/10.1093/treephys/tpt030.
64. Ren, P.; Rossi, S.; Camarero, J.J.; Ellison, A.M.; Liang, E.; Peñuelas, J. Critical temperature and precipitation thresholds for the onset of xylogenesis of *Juniperus przewalskii* in a semi-arid area of the north-eastern Tibetan Plateau. *Ann. Bot.***2017**, *121*, 617–624. htpps://doi.org/10.1093/aob/mcx188.
65. Swidrak, I.; Gruber, A.; Oberhuber, W. Xylem and phloem phenology in co-occurring conifers exposed to drought. *Trees***2014,***28*, 1161–1171. htpps://doi.org/10.1007/s00468-014-1026-x.

606